CrystEngComm

Multimode Crawling Motions of Azobenzene Crystal Induced by Light Intensities for Application as a Shape-Changeable Microcleaner

Journal:	*CrystEngComm*
Manuscript ID	CE-ART-08-2024-000827.R1
Article Type:	Paper
Date Submitted by the Author:	23-Sep-2024
Complete List of Authors:	Saikawa, Makoto; University of Tsukuba, ; National Institute of Advanced Industrial Science and Technology Tsukuba Center Tsukuba Central, Manabe, Kengo; National Institute of Advanced Industrial Science and Technology Tsukuba Center Tsukuba Central, Research Institute for Advanced Electronics and Photonics Saito, Koichiro; National Institute of Advanced Industrial Science and Technology Tsukuba Center Tsukuba Central, Electronics and Photonics Research Institute Kikkawa, Yoshihiro; National Institute of Advanced Industrial Science and Technology (AIST), Norikane, Yasuo; National Institute of Advanced Industrial Science and Technology Tsukuba Center Tsukuba Central,

ARTICLE

Multimode Crawling Motions of Azobenzene Crystal Induced by Light Intensities for Application as a Shape-Changeable Microcleaner

Received 00th January 20xx,
Accepted 00th January 20xx

DOI: 10.1039/x0xx00000x

Makoto Saikawa,[ab] Kengo Manabe,[b] Koichiro Saito,[b] Yoshihiro Kikkawa [b] and Yasuo Norikane*[bc]

Crystals of *trans*-3,3'-dimethylazobenzene (DMAB) exhibit crawling motion on solid surface upon simultaneous exposure to ultraviolet (UV) and visible light from opposite directions. In this study, the shape and velocity during the photoinduced crawling motion of DMAB crystals are successfully controlled by irradiation light intensities. A higher intensity of the visible light than the UV light causes the crystals to be spread shape and move slower (~1 μm min^{-1}). In contrast, a stronger UV light allows them to be droplet-like shape and move faster (~4 μm min^{-1}). The shape and velocity can be varied by adjusting the light intensities. Shape transformation is effectively applied to cargo capture–carry–release tasks. In particular, spread-shaped crystals capture silica particles over a wide area, whereas droplet-like crystals gather and transport them. This result suggests that a multifunctional soft transporter composed of a single component does not require complex fabrication, thereby contributing to the fields of soft robotics and microfluidics.

Introduction

Dynamic organic crystals,[1] whose actuations are triggered by light, are an indispensable class of materials for the development of soft actuators[2] owing to their rapid response time,[3] large Young's modulus,[4] availability of structural analysis through X-ray diffraction,[5] and use of an environmentally friendly energy source.[6] To date, different types of actuations, such as bending,[3,7–11] breaking,[12–15] twisting,[16,17] and peeling,[18–20] have been discovered. Some of those actuations can be performed continuously.[21,22] These shape deformations enable organic crystals to perform specific tasks. For example, a bending motion can lift[3,8,9] and manipulate[10,11] objects, whereas a breaking motion can release encapsulated content.[14,15]

Modulating the motion of crystals using only light stimulus broadens the range of application for crystal-based soft actuators, since light has advantages of contactless and spatiotemporally controllable nature, as well as readily adjustable features, such as wavelength, intensity, and polarization.[23] Several modulation methodologies have been reported by controlling irradiation light. Kobatake et al. demonstrated that the bending angle of photochromic diarylethene crystals can be modulated by exploiting the variations in the light penetration depth with the polarization angle.[24] Other examples of modulating the photoinduced motion include tuning the irradiation wavelength,[25,26] intensity,[27] direction,[28] site,[29] time,[30,31] and temperature.[32] However, the crystal motion modulated by light stimulus has been limited to bending, twisting, and breaking. Additionally, these motions lose continuity and reversibility when the crystals break or when the molecular reorientation that induces their motion reaches an equilibrium state.

In contrast, crystals of certain azobenzene derivatives exhibit continuous photoinduced crawling motion on solid surfaces.[33,34] In particular, crystals of *trans*-3,3'-dimethylazobenzene (DMAB, Fig. 1a) exhibit crawling motion when simultaneously irradiated with ultraviolet (UV, 365 nm) and visible (465 nm) light from opposite directions (Fig. 1b).[33] Exposure to UV light triggers photoisomerization from the *trans* to the *cis* isomer, leading to the melting of the crystals (photomelting). In contrast, visible light induces reverse isomerization from the *cis* to the *trans* isomer, promoting the recrystallization of the crystal. The nonequilibrium state, where photomelting and recrystallization coexist in the crystal, is thought to drive the crawling motion. The motion persists under continuous light irradiation. The mechanism of this motion was explained in detail in our previous paper.[35] The crawling motion facilitates the transport of cargo through remote manipulation using light.[36,37] Recently, we proposed the concept of a photo-controllable microcleaner, in which DMAB crystals successfully performed a series of capture–carry–release tasks for silica particles during crawling motion.[37] The efficiency of microcleaner operation was increased with the use of a surface of a siloxane-based hybrid film (Hyb10, Fig. 1c), which was found to be more suitable for performing tasks than a

[a] Graduate School of Science and Technology, University of Tsukuba, Tsukuba, Ibaraki 305-8571, Japan
[b] Research Institute for Advanced Electronics and Photonics, National Institute of Advanced Industrial Science and Technology (AIST), Tsukuba, Ibaraki 305-8565, Japan. E-mail: y-norikane@aist.go.jp
[c] Faculty of Pure and Applied Sciences, University of Tsukuba, Tsukuba, Ibaraki 305-8571, Japan
† Electronic Supplementary Information (ESI) available. See DOI: 10.1039/x0xx00000x

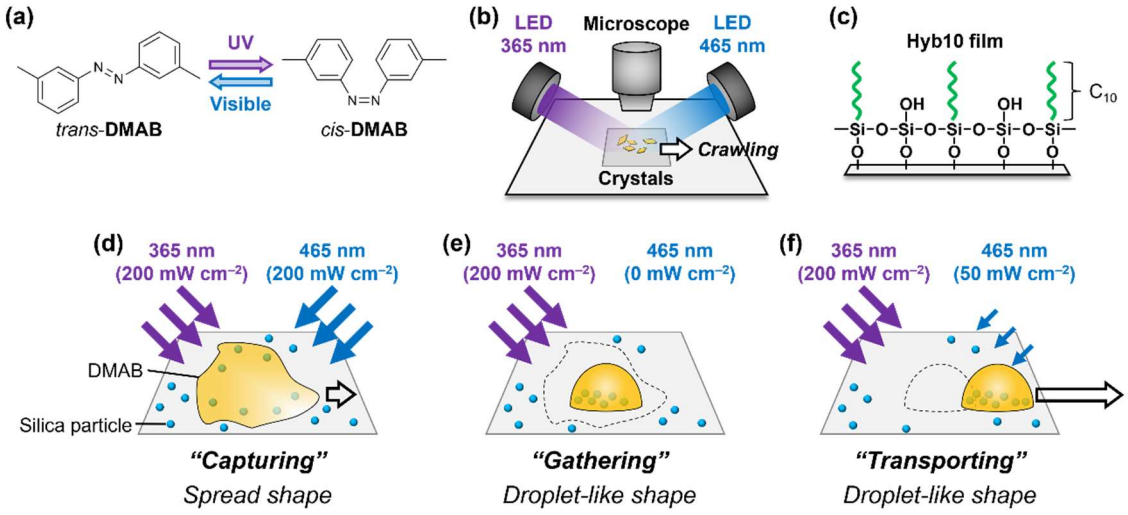

Fig. 1 (a) Chemical structure and photoisomerization of DMAB. (b) Schematic illustration of the experimental setup for observing the crawling motion of DMAB crystals. (c) Schematic illustration of the siloxane-based hybrid film used in this study. Schematic illustrations of the (d) capturing task, (e) gathering task, and (f) transporting task of the silica particles using DMAB crystals.

conventional hydrophobic film with alkyl chains (TMS10). This finding can be ascribed to the small contact angle hysteresis ($\Delta\theta_{cos}$) of the Hyb10 film, which increased the crawling rate without significant shape deformation. Regarding droplet wettability on a solid surface, a smaller contact angle hysteresis contributes to better droplet removability. Compared with the TMS10 film ($\Delta\theta_{cos}$ = 0.21), the surface alkyl chains of the Hyb10 film can rotate or move freely, resulting in a smaller contact angle hysteresis ($\Delta\theta_{cos}$ = 0.09).[37]

Previous studies have only reported approaches that modify the substrate surface in contact with the crystals to modulate crawling motion.[35,37,38] However, the use of light stimuli alone to modulate the crawling motion of organic crystals has not been explored. We anticipated that modulating the morphology and velocity could contribute to the fields of soft robotics and microfluidics, particularly by improving the capture, carry, and release processes of our photo-controllable microcleaner.

Herein, we report a crystal-based soft actuator that can vary its shape and velocity during a photoinduced crawling motion. The shape and velocity of the DMAB crystals varied based on the irradiation intensity. Multimode crawling motions were observed, that is, slower crawling with a spread-shaped crystal and faster crawling with a droplet-like crystal, by simply controlling the relative irradiation intensities of UV and visible light. The changes in the shape and velocity were repeated at least five times. Based on these results, we propose a concept of shape-changeable microcleaner, which can capture, gather, and carry microparticles by transforming its shape for different purposes (Fig. 1d–f).

This study successfully demonstrates the modulation of the shape and velocity of DMAB crystals by controlling the irradiation intensities, which was not achieved previously. The resulting multimode crawling motions enable an improved microcleaner capable of changing shape to efficiently perform each step of the capture and transport processes. This on-demand shape change and sequential application exemplify the successful control of the crawling motion of organic crystals, enabling them to extend the functions of crystals with dynamic motions.

Experimental

DMAB, decyltrimethoxysilane, and tetramethoxysilane were purchased from Tokyo Chemical Industry Co., Ltd. Unless otherwise noted, all other solvents and reagents were purchased from Kishida Chemical Co., Ltd. Hydrochloric acid was used after diluting with water. DMAB was purified by silica-gel column chromatography using ethyl acetate/n-hexane (1:40) and subsequent recrystallization from methanol. The absorption spectra of *trans*- and *cis*-DMAB are shown in Fig. S1 (ESI†). All other reagents were used as received. The silica gel used for column chromatography was purchased from Kanto Chemical Co. Inc. (Silica Gel 60N (spherical, neutral, 40–50 μm)). Silica particles with a diameter of 2 μm were purchased from Ube Exsymo Co., Ltd. (HIPRESICA TS N3N) and used as received.

Cover glasses (Matsunami Glass Ind., Ltd., square microscope cover glass No. 1, 18 mm × 18 mm, thickness: 0.12–0.17 mm) were used as substrates. They were cleaned using a UV/ozone cleaner (Nippon Laser & Electronics Lab). The Hyb10 film was prepared as described in the literature.[37] The TMS10 film was prepared by spin-coating (3,000 rpm for 45 s) onto a cover glass with a solution of the corresponding silane reagents (1 vol% solution in ethanol) and then curing on a digital hot stirrer (AS ONE Corporation, DP-1S) at 100 °C for 10 min. Spin coating was performed using a spin coater (Mikasa Co., Ltd., 1H-D7).

Polycrystals of *trans*-DMAB were ground by using a mortar and pestle and scattered on the substrate through a stainless-steel sieve (mesh size: 25 μm) to place similarly sized crystals without disturbing the substrate surface. This method was

found to be suitable for sample preparation in our previous paper.[35] To prepare a random sample for the transport of the silica particles, the particles and substrate were placed in a glass vial. The particles were placed on the substrate by blowing air. The DMAB crystals were then placed as described earlier.

The motion of the crystals on each substrate was evaluated by light irradiation with light-emitting diodes (LEDs) at 365 nm (CCS Inc., HLV-24UV365-4WNRBTNJ) and 465 nm (CCS Inc., HLV2-22BL-3 W) using the experimental setup described in our previous report.[37] The lights were placed at an angle of 30° with the plane of the substrate and faced each other. The distances between the sample and light source were 2.3 cm for the 365 nm light source and 6.3 cm for the 465 nm light source. Light intensity was monitored using a Newport 1917-R optical power meter equipped with an 818-ST2-UV photodetector. The motion of the crystals was observed at 658 nm using a KEYENCE VK-X150 laser microscope. Photomicrographs were obtained every minute, except during the cargo transport (every 2 min). The travel distance (displacement) and velocity of the crystal motion were measured based on the crystal center, which was defined as the centroid of each image. The motions of the crystals under optically polarized conditions were observed using an Olympus BX51 microscope.

Results and discussion

Crawling motion with spread-shaped crystals

Crystals of DMAB require simultaneous and continuous irradiation of UV (365 nm) and visible (465 nm) light from opposite directions to generate a crawling motion on solid surfaces.[33] The shape and velocity of the crystals during crawling are affected by the surface properties of the substrate, such as its hydrophilicity or hydrophobicity.[35,38] We recently demonstrated the highest velocity of DMAB crystals while maintaining a droplet-like shape on hydrophobic surfaces with an extremely small contact angle hysteresis.[37] In our previous studies, UV (365 nm) and visible (465 nm) light intensities were fixed at 200 and 50 mW cm^{-2}, respectively. In this study, intensified visible light greatly affects the shape and velocity of DMAB crystals during crawling.

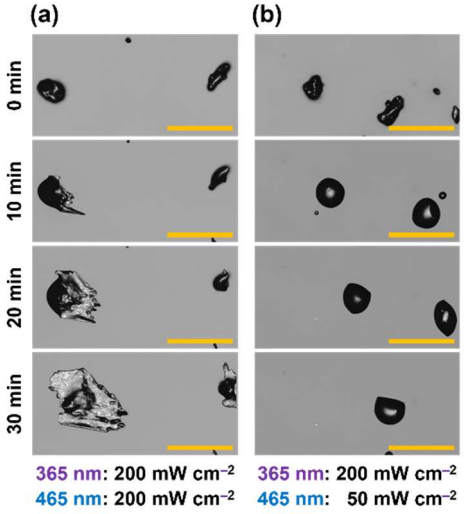

Fig. 2 Photomicrographs of the crawling motion of DMAB crystals on the Hyb10 film after irradiation for t = 0, 10, 20, and 30 min. Light irradiation was performed from the left for UV (365 nm) light and from the right for visible (465 nm) light. The intensities of 365 and 465 nm were (a) 200 and 200 mW cm^{-2} and (b) 200 and 50 mW cm^{-2}, respectively. Scale bar: 100 μm.

Table 1 Average travel distance, velocity, and area of DMAB crystals irradiated with UV and visible light (Ave. ± S.D.)

Surface	Intensities (365–465 nm) / mW cm^{-2}	Travel distance / μm	Velocity / μm min^{-1}	Area[a]
Hyb10[b]	200–200	29 ± 13	1.0 ± 0.4	331 ± 162
	200–50	99 ± 55[b]	4.2 ± 1.7[b]	123 ± 39
TMS10[b]	200–200	15 ± 12	0.5 ± 0.4	267 ± 161
	200–50	63 ± 43[b]	2.5 ± 1.5[b]	183 ± 49

[a] Calculated using the initial crystal area of 100. [b] Ref 37.

Polycrystals of *trans*-DMAB were randomly placed on a Hyb10 surface and exposed to UV and visible light at intensities of 200 and 200 mW cm^{-2}, respectively. During irradiation, almost all crystals in the field of view moved away from the UV light source (Fig. 2a, Fig. S2 and S3 and Movie S1, ESI†). In particular, the crystal center moved to a distance of 29 ± 13 μm in 30 min with the average velocity calculated to be 1.0 ± 0.4 μm min^{-1}. The crystals deformed and spread as they moved. Assuming an initial area of 100 for the crystal, which was projected onto the substrate surface, the average area increased to 331 ± 162 after irradiation for 30 min. The travel distance, velocity, and area were significantly different from those of DMAB crystals irradiated with UV and visible light with intensities at 200 and 50 mW cm^{-2}, respectively, on Hyb10 (Fig. 2b and Table 1). With higher visible-light intensity, the velocity decreases by approximately a quarter, and the area increases by approximately 2.7 times. Therefore, the shape and velocity of the DMAB crystals could be controlled by simply adjusting the irradiation intensity.

Dependence of crawling motion on irradiation light intensities

The dependence of the shape and velocity of the DMAB crystals on the irradiation light intensity was investigated in detail. Crystals of DMAB on the Hyb10 film were exposed to various light intensities in the range of 0–250 mW cm^{-2} for the 365 nm UV light and 0–200 mW cm^{-2} for the 465 nm visible light. The average velocity was plotted against the irradiation intensity, as shown in Fig. 3. When the crystals were exposed only to UV light, they adopted a droplet-like shape and did not move. When exposed to visible light alone, the crystals did not exhibit any crawling motion. However, with the irradiation of the UV-light intensity of 100 mW cm^{-2} or higher and simultaneous irradiation of UV and visible light, the crystals exhibit crawling motion in almost all cases. Moreover, the velocity increases with increasing UV-light intensity. In contrast, the velocity decreases with increasing visible-light intensity. The maximum moving velocity of 4.2 ± 1.7 μm min^{-1} is achieved with the

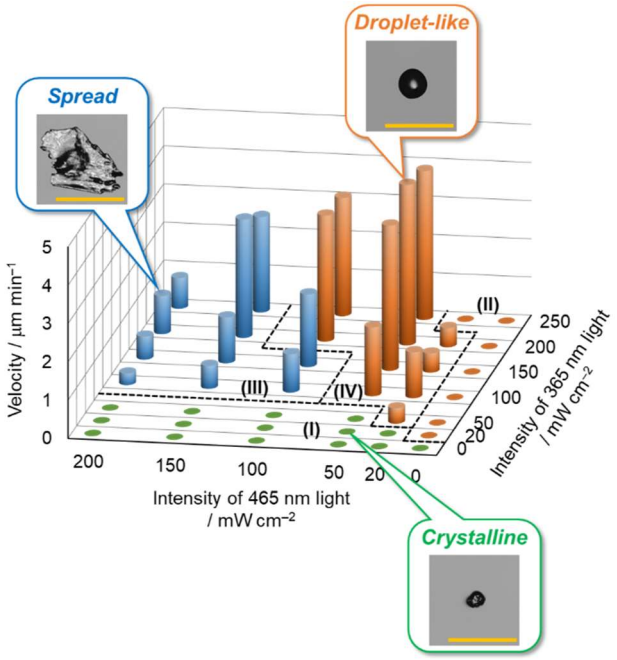

Fig. 3 Average velocity against irradiation intensities on the Hyb10 film. The inset photomicrographs show the appearance of DMAB crystal after irradiation for 30 min. The color of each bar (blue, orange, or green) corresponds to the physical attributes indicated in the photomicrographs. Scale bar: 100 μm.

irradiation intensities of 200 and 50 mW cm^{-2} for UV and visible light, respectively.

Upon exposure to varying UV and visible-light intensities, three distinct shapes are observed: spread-shaped, droplet-like, and crystalline (Fig. 3, Fig. S4 and S5, ESI†). The spread shape depicts significant deformation and irregularly shaped DMAB crystals that appear to wet the substrate. Meanwhile, the droplet-like shape indicates that the DMAB crystals resemble droplets that are mostly round and include elliptical or rod-shaped structures. As revealed by polarized optical microscopy (POM) in a previous study, this shape indicates a mixture of crystals and liquid.[37] Therefore, we used the term "droplet-like," rather than "droplet." The crystalline shape indicates a morphology that initially appeared craggy and maintained its original form even after light irradiation. The relative areas of the crystals after 30 min of irradiation, projected onto the substrate surface with the initial crystal area set to 100, were plotted against the irradiation intensities (Fig. S6, ESI†). At a UV-light intensity of 50 mW cm^{-2} or lower, DMAB crystals mostly retained their crystalline shapes. Owing to sublimation, these areas are smaller than the initial area of 100. Droplet-like shapes are observed when the UV-light intensity is higher than the visible-light intensity. A spread shape appears when the intensity of the visible light is almost equal to or greater than that of the UV light. As the area increased and the spread shape became more pronounced, the travel distance and average velocity decreased.

To determine whether the light intensity dependence was substrate- or crystal-derived, we measured the crawling motion on the TMS10 film, which is a conventional hydrophobic surface,[37] instead of on the Hyb10 film, which is a hydrophobic surface with a small contact angle hysteresis. Crystals of DMAB also exhibited a crawling motion on the TMS10 film. Similar to Hyb10, the shape and velocity vary with the irradiation intensity (Table 1, Fig. S7, S8, Movie S2, ESI†). This suggests that the dependence is mainly ascribed to the nature of the moving crystals, rather than the surface properties of the substrate. POM was used to observe an actual crystal and liquid mixture during motion to investigate the moving crystals in detail. POM revealed a birefringence in the spread-shaped DMAB crystals irradiated with UV and visible light at intensities of 200 and 200 mW cm^{-2} on the Hyb10 film (Fig. 4b, Fig. S9, ESI†). The spread-shaped DMAB is highly occupied by the actual crystal. In contrast, it seemed that the droplet-like DMAB, irradiated with UV and visible light at intensities of 200 and 50 mW cm^{-2}, is surrounded by a certain amount of liquid (Fig. 4c).[37] Thus, this observation indicated that the ratio of crystal to liquid differed with the visible-light intensity.

A mechanism for the dependence of properties on the light intensity was proposed by considering the ratio of the actual crystal volume to the total volume of the crystal–liquid mixture.

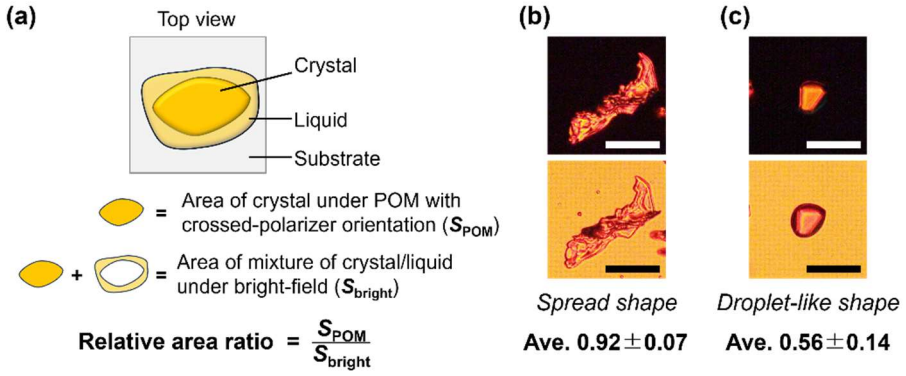

Fig. 4 (a) A schematic illustration of the calculation method of the relative area ratio of the actual crystal area to the total area occupied by the crystal/liquid mixture. (b, c) Photomicrographs of the DMAB crystals on the Hyb10 film after irradiation for 30 min. The intensities of the 365 nm UV and 465 nm visible light were (b) 200 and 200 mW cm^{-2} and (c) 200 and 50 mW cm^{-2}, respectively. The top photographs were captured under a polarizing optical microscope with a crossed-polarizer orientation and the bottom photographs were taken under a bright-field microscope. The values below the photographs show the average relative area ratio. Scale bar: 50 μm.

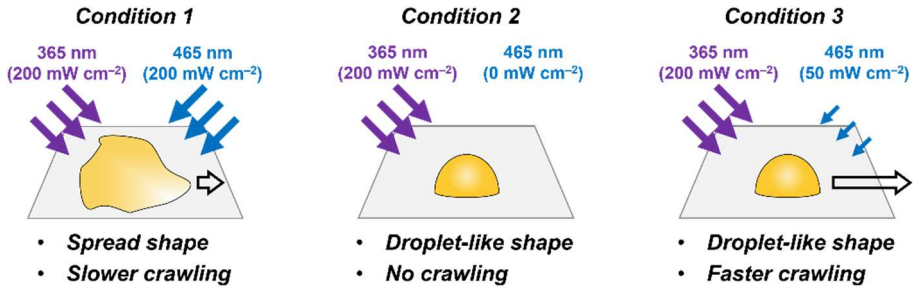

Fig. 5 Schematic illustrations of DMAB crystals upon light exposure under each irradiation condition.

We anticipated that this ratio would differ for the spread-shaped and droplet-like DMAB crystals owing to the variations in light intensity. However, quantifying the crystal volume is difficult because it requires the three-dimensional observation of actual DMAB crystals under a crawling motion. Thus, the ratio of the actual crystal area to the total area occupied by the crystal/liquid mixture projected onto the substrate was estimated. The relative ratio was determined by dividing the area of the actual crystals estimated by POM (S_{POM}) by the area of the crawling DMAB crystal obtained using a bright-field microscope (S_{bright}, Fig. 4). The average area ratio of the spread-shaped crystal (0.92 ± 0.07) is larger than that of the droplet-like crystal (0.56 ± 0.14). These results indicate that the spread-shaped DMAB crystal has a higher ratio of the actual crystal volume to the total volume of the crystal/liquid mixture.

As a crawling motion mechanism, we consider that liquefied DMAB crystals melted by UV light is supplied from the back (UV-light-source side) to the front (visible-light-source side) of the crystal, followed by recrystallization and crystal growth in the direction of the visible-light source. This nonequivalent state is the driving force that propels crystal crawling.[35] In this study, the balance between melting and recrystallization determined the shape and velocity of the crystals under light irradiation, as they depend on the UV and visible-light intensities. Much stronger visible light or the absence of UV light (region I shown in Fig. 3) causes negligible melting and minimal changes in the crystal shape, whereas much stronger UV light or the absence of visible light (region II shown in Fig. 3) results in complete melting and a droplet-like shape. These two situations do not result in a nonequilibrium state or produce a crawling motion. When the visible light was relatively stronger than the UV light (region III shown in Fig. 3), the liquefied DMAB crystal rapidly recrystallized before it migrated forward, resulting in a spread shape, because the movement of the surface layer of the crystals could not be followed by the internal crystals. Conversely, when the UV-light intensity was greater than that of the visible light (region IV shown in Fig. 3), the recrystallization rate was moderate to move the liquefied DMAB crystals to the front of the crystal, facilitating the movement of the surface layer of the crystals followed by the internal crystals, resulting in droplet-like crystals with a higher velocity.

Repeatable change of shape and velocity

We attempted to control the shape and velocity of the crystals by varying the light intensity under three irradiation conditions. Condition 1 involved irradiation with UV and visible light at 200 and 200 mW cm^{-2} for 20 min, resulting in a spread shape and slower crawling motion. Condition 2 entailed irradiation with UV light at 200 mW cm^{-2} for 2 min, resulting in a droplet-like shape without crawling motion. Condition 3 involved irradiation with UV and visible light at 200 and 50 mW cm^{-2}, respectively, for 20 min, resulting in a droplet-like shape and faster crawling motion (Fig. 5). Irradiation under conditions 1 and 3 was followed by irradiation under condition 2. The irradiation times of 20 min under conditions 1 and 3 were chosen to adequately observe the changes in crawling motion and facilitate repeated adjustments in the irradiation intensity. In contrast, the

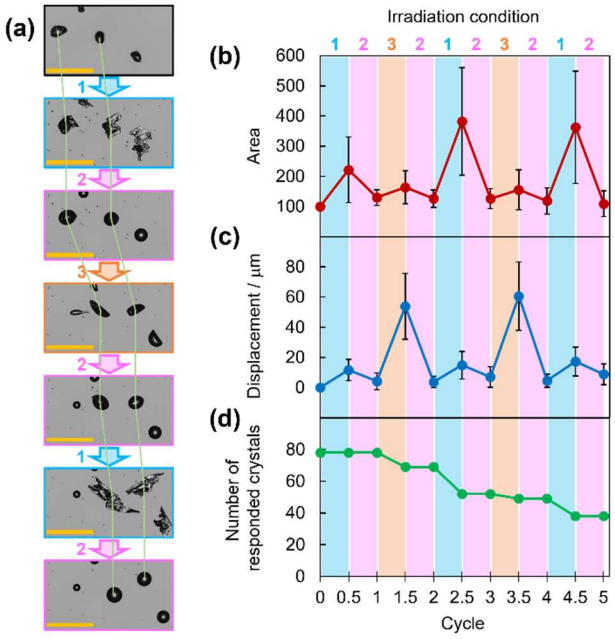

Fig. 6 (a) Photomicrographs of the crawling motion and deformation of DMAB crystals on the Hyb10 film under alternating irradiation conditions. Scale bar: 100 μm. Condition 1: 365 and 465 nm (200 and 200 mW cm^{-2}) of UV and visible light, respectively, for 20 min. Condition 2: 365 nm UV light (200 mW cm^{-2}) for 2 min. Condition 3: 365 and 465 nm (200 and 50 mW cm^{-2}) of UV and visible light, respectively, for 20 min. Light irradiation was performed from the left for UV light (365 nm) and from the right for visible light (465 nm). Changes in (b) area, (c) displacement, and (d) number of responded crystals.

irradiation time under condition 2 was optimized to 2 min to maximize the number of round droplet-like crystals while minimizing the complete melting of the crystals (Fig. S10, Movie S3, ESI†). Consequently, we successfully achieved the on-demand control of the shape and velocity of the crystals (Fig. 6, Movie S4, ESI†). The average area of the crystals decreases after shifting the conditions from conditions 1 to 2. Interestingly, similar results are observed after changing the condition from condition 3 to 2 as the droplet-like shape of some crystals under condition 3 deformed while crawling because of unexpected crystal growth. An obvious contrast in the area and displacement of the crystal center is observed under conditions 1 and 3. Approximately half of the crystals successfully underwent five cycles, with each cycle including the processes of condition 2 once. The number of DMAB crystals responding to light gradually decreases, which can be ascribed to the complete melting of some crystals owing to the UV light exposure under condition 2. The cycles involving condition 1, followed by condition 2, were also successful for five cycles (Fig. S11, Movie S5, ESI†). The area of the crystals in the first spreading process (condition 2) was smaller than those in the second and subsequent spreading processes. This may be the reason why, when switching from conditions 2 to 1, DMAB is a mixture of liquid and crystals. This allowed the crystals to grow more easily than they did during the initial spreading process, starting from a completely crystalline state. In addition, cycles under condition 1 followed by condition 3 were also tested (Fig. S12, Movie S6, ESI†). When transforming from a spread shape into a droplet-like shape, that is, when changing from conditions 1 to 3, the splitting of DMAB into smaller pieces was more pronounced compared to attempts with condition 2. Therefore, condition 2, which involved stopping the crawling motion and transforming the spread shape into a single droplet-like DMAB, was deemed an important step for repetitive cycles.

Application to cargo transport

We recently demonstrated that DMAB crystals were capable of performing a series of capture–carry–release tasks for silica particles during crawling motion.[37] The monodispersed spherical silica particles exhibited good wettability with melted DMAB and were continuously held by the crawling DMAB crystals. In that case, the crystal shape was maintained during the capturing and carrying processes; that is, the crystals could capture particles within the range they passed through but could not capture particles outside of that range owing to the constant width. To improve the capturing process, we expected the spread shape to be more efficient in capturing silica particles over a larger surrounding area than the droplet-like crystals before the carrying process. The duration of light irradiation under condition 1 was optimized in advance. The changes in the area of the crystals over time were tracked (Fig. S13, ESI†). After 60 min of irradiation with UV and visible light at both 200 mW cm^{-2}, the maximum area was almost achieved. After 70 min of irradiation, the area started to decrease owing to the sublimation of the crystals. Therefore, the irradiation time for condition 1 was set to 60 min.

Silica particles with diameters of 2 μm and DMAB crystals were randomly placed on the Hyb10 film and exposed to UV and visible light (Fig. 7, Movie S7, ESI†). At UV and visible-light intensities of 200 and 200 mW cm^{-2} each (condition 1), the DMAB crystals deformed and spread to cover the silica particles. After irradiation for 60 min, the DMAB crystals and silica particles were exposed to UV light at an intensity of 200 mW cm^{-2} (condition 2) for 2 min, prompting the transformation of the spread-shaped crystals to droplet-like crystals. Moreover, no silica particles were left in the area initially covered by the spread-shaped crystals. Thus, the light irradiation under condition 2 can be described as a gathering process of the silica particles and spread-shaped DMAB crystals, introducing a new step in the series of tasks performed by the microcleaner.[37] Subsequently, the droplet-like crystals were exposed to UV and

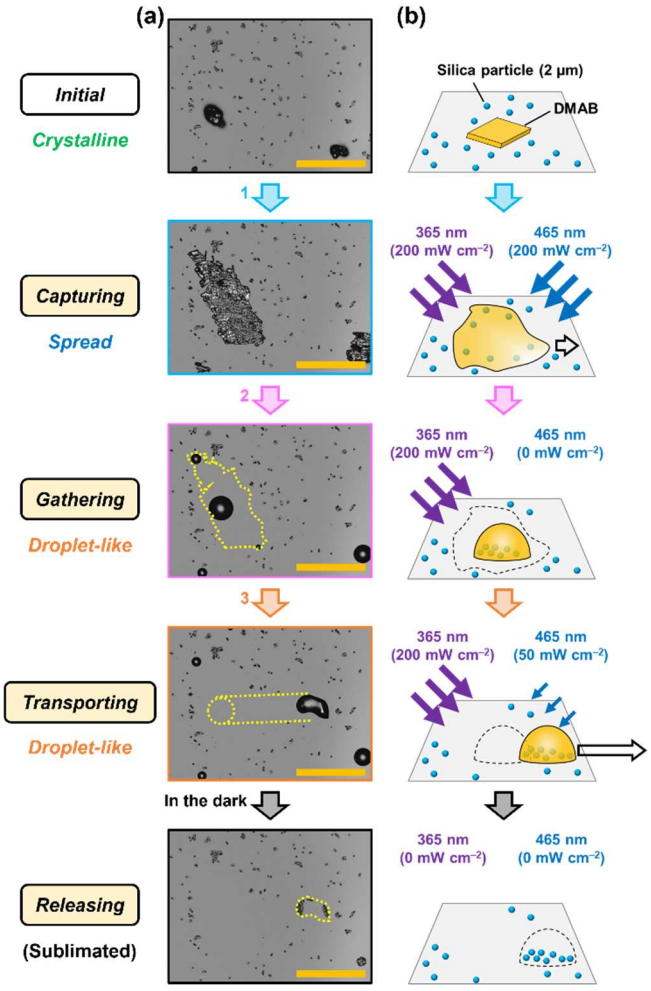

Fig. 7 (a) Photomicrographs and (b) schematic illustrations of the crawling motion of DMAB crystals on the Hyb10 film where silica particles with a diameter of 2 μm were placed under alternating irradiation as described below. Condition 1: 365 and 465 nm (200 and 200 mW cm^{-2}) of UV and visible light, respectively, for 60 min. Condition 2: 365 nm (200 mW cm^{-2}) UV light for 2 min. Condition 3: 365 and 465 nm (200 and 50 mW cm^{-2}) of UV and visible light, respectively, for 30 min. Light irradiation was performed from the left for UV (365 nm) light and from the right for visible (465 nm) light. Scale bar: 100 μm.

visible light at intensities of 200 and 50 mW cm^{-2}, respectively, (condition 3) for 30 min. Most crystals moved away from the UV-light source. After transporting the silica particles, the DMAB crystals were removed via sublimation, leaving the transported silica particles on the substrate. Consequently, the DMAB crystals transformed into a spread shape with a large area when capturing particles, and a droplet-like shape with a high velocity when carrying particles. This significantly improved the capture, transport, and release processes of the DMAB crystal microcleaner. Grabbing[39] and sweeping[40] silica particles using organic crystals have been reported as independent studies. This study demonstrated that DMAB crystals efficiently performed both capturing and transporting silica particles through shape changes induced by light intensities. Conclusions

In this study, we clarified the dependence of the crawling motion of DMAB crystals on the irradiation light intensity in terms of the morphology and velocity. Droplet-like and spread-shaped crystals can be selectively observed and achieved on demand by adjusting the UV and visible-light relative intensities. The droplet-like shape increased the velocity of the crystals (~4 μm min^{-1}), whereas the spread shape decreased the velocity (~1 μm min^{-1}). The balance between photomelting by UV light and recrystallization by visible light determined the shape and velocity of the crystals. In addition, the shape change was successfully applied to make the photo-controllable microcleaner more efficient by improving the capturing process through the spread shape. The shape-changeable microcleaner proposed in this study can transform into a spread shape during the capturing process and into a droplet-like shape during the gathering and carrying processes. In contrast, the microcleaner in our previous study could only adopt a droplet-like shape due to a single irradiation intensity. To the best of our knowledge, this paper first reported multiple shape transformations of organic crystals that has been successfully achieved and applied to perform a series of cargo capture–carry–release tasks using only a light stimulus. This study of DMAB crystals with single components and light-controllable multifunctionality demonstrates potential development on soft robotics, which has been focused on compositing or assembling LCE films. Furthermore, these results highlight the promising prospects of photoinduced crawling crystals in microscale containers, flasks, and reactors, and novel methods for particle assembly.

Author contributions

M.S. conducted the experiments and drafted the manuscript; K.M. helped with the preparation of the substrates; K.M., K.S., and Y.K. reviewed and edited the manuscript; Y.N. guided the work and drafted the manuscript. All authors contributed to the discussion and preparation of the manuscript. All authors have given approval to the final version of the manuscript.

Data availability

The data that support the findings of this study are available within the article and its ESI.† Further data may be requested from the corresponding author upon reasonable request.

Conflicts of interest

There are no conflicts to declare.

Acknowledgements

This work was supported by JSPS KAKENHI (Grant No. JP20H02456, JP21K18860, JP22K14531, JP23H01702, JP23K17822, and JP24K01577); and JST, the establishment of university fellowships towards the creation of science technology innovation (Grant No. JPMJFS2106) and JST SPRING (Grant No. JPMJSP2124). We thank Dr. Toshiko Mizokuro (AIST) for providing the UV/ozone cleaner and spin coater.

Notes and references

1 W. M. Awad, D. W. Davies, D. Kitagawa, J. Mahmoud Halabi, M. B. Al-Handawi, I. Tahir, F. Tong, G. Campillo-Alvarado, A. G. Shtukenberg, T. Alkhidir, Y. Hagiwara, M. Almehairbi, L. Lan, S. Hasebe, D. P. Karothu, S. Mohamed, H. Koshima, S. Kobatake, Y. Diao, R. Chandrasekar, H. Zhang, C. C. Sun, C. Bardeen, R. O. Al-Kaysi, B. Kahr and P. Naumov, *Chem. Soc. Rev.*, 2023, **52**, 3098–3169.
2 I. Apsite, S. Salehi and L. Ionov, *Chem. Rev.*, 2022, **122**, 1349–1415.
3 S. Kobatake, S. Takami, H. Muto, T. Ishikawa and M. Irie, *Nature*, 2007, **446**, 778–781.
4 M. K. Panda, S. Ghosh, N. Yasuda, T. Moriwaki, G. D. Mukherjee, C. M. Reddy and P. Naumov, *Nat. Chem.*, 2015, **7**, 65–72.
5 Y. Zheng, H. Sato, P. Wu, H. J. Jeon, R. Matsuda and S. Kitagawa, *Nat. Commun.*, 2017, **8**, 100.
6 O. S. Bushuyev, M. Aizawa, A. Shishido and C. J. Barrett, *Macromol. Rapid Commun.*, 2018, **39**, 1700253.
7 H. Koshima, N. Ojima and H. Uchimoto, *J. Am. Chem. Soc.*, 2009, **131**, 6890–6891.
8 M. Morimoto and M. Irie, *J. Am. Chem. Soc.*, 2010, **132**, 14172–14178.
9 F. Tong, W. Xu, T. Guo, B. F. Lui, R. C. Hayward, P. Palffy-Muhoray, R. O. Al-Kaysi and C. J. Bardeen, *J. Mater. Chem.*, 2020, **8**, 5036–5044.
10 J. Lee, S. Oh, J. Pyo, J.-M. Kim and J. H. Je, *Nanoscale*, 2015, **7**, 6457–6461.
11 R. Nishimura, A. Fujimoto, N. Yasuda, M. Morimoto, T. Nagasaka, H. Sotome, S. Ito, H. Miyasaka, S. Yokojima, S. Nakamura, B. L. Feringa and K. Uchida, *Angew. Chem., Int. Ed.*, 2019, **58**, 13308–13312.
12 P. Naumov, S. C. Sahoo, B. A. Zakharov and E. V. Boldyreva, *Angew. Chem., Int. Ed.*, 2013, **52**, 9990–9995.
13 K. McGehee, K. Saito, D. Kwaria, H. Minamikawa and Y. Norikane, *Phys. Chem. Chem. Phys.*, 2024, **26**, 6834–6843.
14 E. Hatano, M. Morimoto, T. Imai, K. Hyodo, A. Fujimoto, R. Nishimura, A. Sekine, N. Yasuda, S. Yokojima, S. Nakamura and K. Uchida, *Angew. Chem., Int. Ed.*, 2017, **56**, 12576–12580.
15 A. Nagai, R. Nishimura, Y. Hattori, E. Hatano, A. Fujimoto, M. Morimoto, N. Yasuda, K. Kamada, H. Sotome, H. Miyasaka, S. Yokojima, S. Nakamura and K. Uchida, *Chem. Sci.*, 2021, **12**, 11585–11592.

16 L. Zhu, R. O. Al-Kaysi and C. J. Bardeen, *J. Am. Chem. Soc.*, 2011, **133**, 12569–12575.
17 D. Kitagawa, H. Nishi and S. Kobatake, *Angew. Chem., Int. Ed.*, 2013, **52**, 9320–9322.
18 F. Tong, M. Al-Haidar, L. Zhu, R. O. Al-Kaysi and C. J. Bardeen, *Chem. Commun.* , 2019, **55**, 3709–3712.
19 R. O. Al-Kaysi, US Pat., UV10259941B1, 2019.
20 M. Tamaoki, D. Kitagawa and S. Kobatake, *Cryst. Growth Des.*, 2021, **21**, 3093–3099.
21 F. Tong, D. Kitagawa, I. Bushnak, R. O. Al-Kaysi and C. J. Bardeen, *Angew. Chem. Int. Ed.*, 2021, **60**, 2414–2423.
22 K. Lam, V. Carta, M. Almtiri, I. Bushnak, I. Islam, R. O. Al-Kaysi and C. J. Bardeen, *J. Am. Chem. Soc.*, 2024, **146**, 18836–18840.
23 M. Rey, G. Volpe and G. Volpe, *ACS Photonics*, 2023, **10**, 1188–1201.
24 A. Hirano, D. Kitagawa and S. Kobatake, *CrystEngComm*, 2019, **21**, 2495–2501.
25 S. Hasebe, Y. Hagiwara, K. Hirata, T. Asahi and H. Koshima, *Mater. Adv.*, 2022, **3**, 7098–7106.
26 D. Kitagawa, R. Tanaka and S. Kobatake, *Phys. Chem. Chem. Phys.*, 2015, **17**, 27300–27305.
27 A. Hirano, T. Hashimoto, D. Kitagawa, K. Kono and S. Kobatake, *Cryst. Growth Des.*, 2017, **17**, 4819–4825.
28 D. Kitagawa, H. Tsujioka, F. Tong, X. Dong, C. J. Bardeen and S. Kobatake, *J. Am. Chem. Soc.*, 2018, **140**, 4208–4212.
29 J. De, Q. Liao, X. Xiao, H. Liu, W. Chen, L. Chen, H. Geng, Y. Liao and H. Fu, *ACS Appl. Mater. Interfaces*, 2020, **12**, 27493–27498.
30 T.-Y. Xu, F. Tong, H. Xu, M.-Q. Wang, H. Tian and D.-H. Qu, *J. Am. Chem. Soc.*, 2022, **144**, 6278–6290.
31 P. J. Hazarika, P. Gupta, S. Allu and N. K. Nath, *CrystEngComm*, 2024, **26**, 1671–1676.
32 Y. Hao, S. Huang, Y. Guo, L. Zhou, H. Hao, C. J. Barrett and H. Yu, *J. Mater. Chem.*, 2019, **7**, 503–508.
33 E. Uchida, R. Azumi and Y. Norikane, *Nat. Commun.*, 2015, **6**, 7310.
34 K. Saito, M. Ohnuma and Y. Norikane, *Chem. Commun.*, 2019, **55**, 9303–9306.
35 Y. Norikane, M. Hayashino, M. Ohnuma, K. Abe, Y. Kikkawa, K. Saito, K. Manabe, K. Miyake, M. Nakano and N. Takada, *Front Chem*, 2021, **9**, 684767.
36 K. Saito, K. Ichiyanagi, S. Nozawa, R. Haruki, D. Fan, T. Kanazawa and Y. Norikane, *Adv. Mater. Interfaces*, **10**, 2202525.
37 M. Saikawa, M. Ohnuma, K. Manabe, K. Saito, Y. Kikkawa and Y. Norikane, *Mater. Horiz.*, 2024, DOI: 10.1039/D4MH00455H.
38 Y. Norikane, M. Hayashino, M. Ohnuma, K. Abe, Y. Kikkawa, K. Saito, K. Manabe, K. Miyake, M. Nakano and N. Takada, *Langmuir*, 2021, **37**, 14177–14185.
39 K. Lam, I. Islam, E. Bushnak, R. Al-Muzarie, C. J. Bardeen and R. O. Al-Kaysi, *ChemRxiv*, 2019, preprint, DOI: 10.26434/chemrxiv-2023-69ns9.v1
40 R. O. Al-Kaysi, F. Tong, M. Al-Haidar, L. Zhu and C. J. Bardeen, *Chem. Commun.*, 2017, **53**, 2622–2625.

August 18, 2024

Data Availability Statement

Title: Multimode Crawling Motions of Azobenzene Crystal Induced by Light Intensities for Application as a Shape-Changeable Microcleaner

Authors: Makoto Saikawa, Kengo Manabe, Koichiro Saito, Yoshihiro Kikkawa, and Yasuo Norikane*

The data that support the findings of this study are available within the article and its Supplementary Information files. Further data may be requested from the corresponding author upon reasonable request.